Solid State Communications 152 (2012) 616–620

Contents lists available at SciVerse ScienceDirect

Solid State Communications

journal homepage: www.elsevier.com/locate/ssc

Ba^{2+} doping effect on the charge ordering of $Bi_{0.5}Sr_{0.5-x}Ba_xMnO_3$ ($x = 0$–0.30)

Renwen Li [a,b], Li Pi [a,*], Yuheng Zhang [a]

[a] High Magnetic Field Laboratory, Chinese Academy of Sciences and University of Science and Technology of China, Hefei 230031, People's Republic of China

[b] Department of Physics and Electronic Engineering, Hefei Normal University, Hefei 230061, People's Republic of China

ARTICLE INFO

Article history:
Received 28 September 2011
Received in revised form
28 November 2011
Accepted 5 January 2012
by T. Kimura
Available online 15 January 2012

Keywords:
A. Perovskite manganites
D. Charge ordering
E. Ba doping

ABSTRACT

Polycrystalline samples of Ba-doped $Bi_{0.5}Sr_{0.5}MnO_3$ have been prepared by a standard solid-state reaction. The influence of the Ba doping effect on the structural, macro-magnetic, and micro-magnetic properties of the compounds has been investigated experimentally. All the samples crystallize in an orthorhombic structure and the lattice parameters increase continuously with increasing Ba doping level. Due to the increase of the e_g electron bandwidth resulting from the Ba doping, the charge-ordering (CO) transition temperature T_{CO} decreases noticeably. Both the macro-magnetic and the micro-magnetic data show that, in all the samples, only a paramagnetic (PM)/charge-disordered state exists above the CO transition, and only a charge-ordered state coexists with the PM matrix below the CO transition, while an antiferromagnetic (AFM) state coexists with a ferromagnetic (FM) state and a paramagnetic (PM) state at temperatures below the Néel temperature (T_N).

1. Introduction

Perovskite manganites $Ln_{1-x}A_xMnO_3$ (Ln = rare earth, A = alkaline earth) have attracted great attention because of their rich physics in electronic and magnetic properties including metal–insulator transition, ferromagnetic (FM) to paramagnetic (PM) phase change, and charge ordering (CO) [1–10].

It is known that ferromagnetism requires the delocalization of e_g electrons over the background of localized parallel t_{2g}^3 core spins along the Mn^{3+}–O–Mn^{4+} network by double-exchange (DE) interaction [11], while CO is realized by the localization of e_g electrons at the Mn^{3+} and Mn^{4+} sites and the ordering of these ions in a particular pattern [12]. It is believed that the orbital overlapping between neighboring ions will be affected by the Mn^{3+}/Mn^{4+} ratio and the Mn–O–Mn bond angle. This will affect the mobility of the itinerant e_g electron and strongly influence the CO state of manganese oxides [1]. However, most research has focused on the lanthanide manganites, and the non-lanthanide manganites are relatively rarely studied. $Bi_{1-x}Sr_xMnO_3$ is a typical system that exhibits a CO transition with charge-ordering temperature T_{CO} as high as ~500 K for a wide range of x values [13–28]. Compared with lanthanide ions, Bi^{3+} ions have highly polarizable $6s^2$ lone pairs [29], which make bismuth-based manganites always to have a peculiar lattice distortion. The one-electron bandwidth (W) tuning mechanism has been widely used to quantitatively justify the CO temperature variation in the perovskite manganites [30], and the W value can be controlled by varying the Mn–O–Mn bond angle and Mn–O bond length through the change of the average ionic radius $\langle r_A \rangle$ of A-site cations [31]. In the $Bi_{0.5}Sr_{0.5}MnO_3$ system, the CO phenomenon occurs at ~475 K [32], which is approximately 300 K above the temperature predicted by the bandwidth tuning mechanism in the $Ln_{0.5}(Ca, Sr)_{0.5}MnO_3$ family. This transition also takes place ~150 K above that in $Bi_{0.5}Ca_{0.5}MnO_3$, which is much more distorted. Strikingly, according to Kirste et al. and García-Muñoz et al. [26,32], the T_{CO} variation along the $Bi_{0.5}(Sr_{1-y}Ca_y)_{0.5}MnO_3$ series ($0 < y < 1$) is not monotonic, but T_{CO} suddenly jumps 150 K for $y \sim 0.5$ compositions. Based on their synchrotron, neutron powder diffraction (NPD), and magnetization data, they proposed a mechanism that the manifestation of the $6s^2$ character of the Bi^{3+} lone pair seems to be weakly screened to favor charge ordering for $Bi_{0.5}(Sr_{1-y}Ca_y)_{0.5}MnO_3$ with high Sr content.

Since Ca, Sr, and Ba all belong to the alkaline-earth family, one natural issue is that how the properties of $Bi_{0.5}Sr_{0.5}MnO_3$ evolve upon larger Ba^{2+} substituting Sr^{2+}. In this work, we choose then $Bi_{0.5}Sr_{0.5-x}Ba_xMnO_3$ series to investigate the Ba doping effect on the structure and magnetic properties. Experimental results show that, upon substitution of the Ba^{2+} ion for the Sr^{2+} ion with $x < 0.30$, the structural symmetry keeps its orthorhombic structure with the *Pnma* space group, but the CO state decreases noticeably, due to the widened bandwidth. Both the macro-magnetic and the micro-magnetic data show that, in all the samples, only a charge-ordered state coexists with a PM/charge-disordered matrix below T_{CO}, while an antiferromagnetic (AFM) state coexists with an FM state and a PM state at temperatures below the Néel temperature (T_N).

* Corresponding author. Tel.: +86 5513600470; fax: +86 5513600470.
E-mail address: pili@ustc.edu.cn (L. Pi).

0038-1098/$ – see front matter © 2012 Elsevier Ltd. All rights reserved.
doi:10.1016/j.ssc.2012.01.014

Table 1
Structural parameters obtained by Rietveld refinement of X-ray diffraction data of $Bi_{0.5}Sr_{0.5-x}Ba_xMnO_3$ ($x = 0$–0.20) samples at room temperature. Space group *Pnma*. ⟨Mn–O⟩ is the average Mn–O bond length. ⟨Mn–O–Mn⟩ is the average Mn–O–Mn bond angle. W is the empirical value of the bandwidth for ABO_3-type perovskites using the tight-binding approximation [37]: $W \propto \cos\omega/(\langle Mn\text{–}O\rangle)^{3.5}$, where $\omega = 0.5(\pi - \langle Mn\text{–}O\text{–}Mn\rangle)$.

Parameter	$x = 0$	$x = 0.05$	$x = 0.10$	$x = 0.15$	$x = 0.20$
a (Å)	5.55063 (23)	5.55470 (27)	5.55716 (21)	5.56671 (15)	5.56542 (18)
b (Å)	5.54671 (30)	5.55816 (18)	5.56058 (27)	5.56638 (22)	5.56683 (28)
c (Å)	7.63980 (43)	7.65657 (41)	7.67951 (37)	7.66485 (25)	7.69968 (30)
V (Å^3)	235.212 (21)	236.388 (19)	237.305 (18)	237.506 (14)	238.549 (17)
⟨Mn–O⟩ (Å)	1.988 (3)	1.985 (3)	1.974 (0)	1.953 (8)	1.967 (6)
⟨Mn–O–Mn⟩ (°)	155.65 (10)	157.30 (15)	162.30 (16)	172.40 (16)	166.60 (24)
W ($*10^{35}$)	0.08819	0.08892	0.09143	0.09571	0.09294
σ^2 (Å^2)	0.00490	0.00724	0.00944	0.01152	0.01348

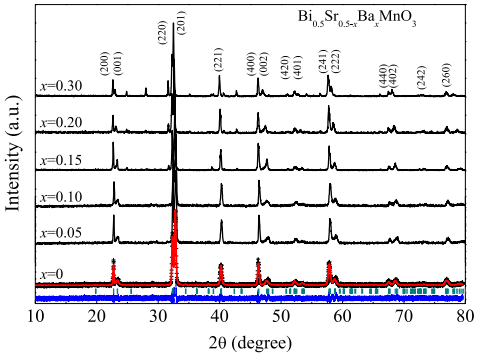

Fig. 1. (Color online) Room-temperature X-ray-diffraction patterns of $Bi_{0.5}Sr_{0.5-x}Ba_xMnO_3$ ($x = 0$, 0.05, 0.10, 0.15, 0.20, and 0.30) samples. The solid red curve is the fit for $x = 0$ from the Rietveld refinement using GSAS. The vertical marks indicate the positions of Bragg peaks and the bottom curve shows the difference between the observed and calculated intensities.

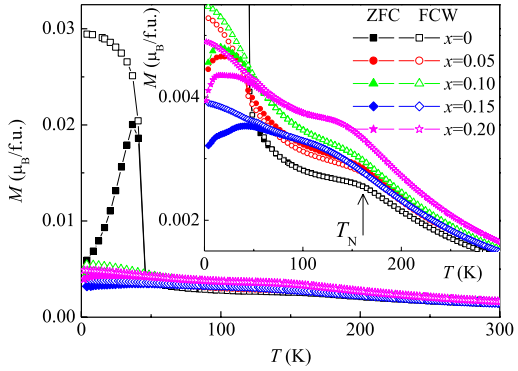

Fig. 2. (Color online) Temperature dependence of magnetization for $Bi_{0.5}Sr_{0.5-x}Ba_xMnO_3$ ($x = 0$, 0.05, 0.10, 0.15, and 0.20) samples in ZFC (solid) and FCW (open) sequences below 300 K. The applied field is 0.05 T. The inset shows an enlarged view.

2. Experiment

Polycrystalline samples of $Bi_{0.5}Sr_{0.5-x}Ba_xMnO_3$ with $x = 0$, 0.05, 0.10, 0.15, 0.20, and 0.30 were prepared by the conventional solid-state reaction method. Stoichiometric proportions of high-purity Bi_2O_3(99.99%), $SrCO_3$(99.99%), $BaCO_3$(99.99%), and MnO_2(99.9%) were mixed and heated at 800 °C for 24 h and 900 °C for 24 h in air with several intermediate grindings. Finally, they were pelletized, and then sintered in air at 1000 °C for 24 h. Powder X-ray diffraction (XRD) measurements were carried out using a Rigaku-TTR3 X-ray diffractometer using high-intensity Cu Kα radiation at room temperature. The crystal structure refinement was made using the Rietveld technique with the program GSAS. The magnetic measurements were performed using a Quantum Design MPMS system. The electron spin resonance (ESR) spectra were collected with a Bruker BioSpin's EPR EMXplus spectrometer at 9.30 GHz.

3. Results and discussion

Fig. 1 shows the room-temperature XRD patterns of the $Bi_{0.5}Sr_{0.5-x}Ba_xMnO_3$ ($x = 0$–0.30) samples. It indicates that all the samples except for the $x = 0.30$ sample are single phase with no obviously detectable impurity phases. All diffraction peaks can be indexed to an orthorhombic lattice with the space group *Pnma*. The lattice parameters can be obtained by fitting the experimental data using the standard Rietveld technique [33]. In the process of refinement, the substitution of Ba ions at Sr sites was considered. Detailed results of the unit cell parameters a, b, c, and cell volume V versus Ba doping content x are shown in Table 1. One can see that, with Ba^{2+} substituting Sr^{2+}, all of the a, b, and c parameters increase and the cell volume expands, which indicates that the larger Ba^{2+} ions are indeed substituted in the Sr^{2+} sites.

Fig. 2 shows the magnetization against temperature ($M(T)$) curves for the samples under 0.05 T in a zero-field-cooled warming (ZFC) sequence and field-cooled warming (FCW) sequence below 300 K. Fig. 3 shows the temperature dependence of the magnetization $M(T)$ and its inverse $M^{-1}(T)$ curves for the samples under 0.05 T in a warming sequence and a cooling sequence above 300 K. As shown in Figs. 2 and 3(a), the $M(T)$ curves for $x = 0$, i.e., $Bi_{0.5}Sr_{0.5}MnO_3$, exhibit three distinct deviations: the first deviation at $T_{CO} \sim 490$ K, defined as the bifurcation between the warming and cooling curves or the sudden change in the slope of the $M^{-1}(T)$ curve, corresponds to the onset of orbital ordering and charge ordering (OO/CO) [27,32]; the second, at $T_N \sim 150$ K, corresponds to a transition from FM interactions between Mn ions driven by double exchange to AFM interactions driven by superexchange interactions; the third, at ~40 K, is a lambda-shape anomaly, suggesting a spin-glass-like state transition. The result for $Bi_{0.5}Sr_{0.5}MnO_3$ here is consistent with the previous reports [14,19,21,23,28,32,34–36]. The $M(T)$ and $M^{-1}(T)$ curves for Ba-doped samples demonstrate similar behavior as the matrix. But, as shown in Fig. 3, the Ba doping leads to an obvious decrease of T_{CO} to lower temperature, and, for $x = 0.30$, the deviation almost disappears, implying a reduction of CO due to the Ba doping. The variation of T_{CO} versus Ba doping content x is shown in the left axes Fig. 4. Besides, Fig. 2 also shows a slightly decrease of the AFM transition temperature, suggesting a weakening of AFM coupling due to the Ba doping. The variation of T_N versus Ba doping content x is shown in the right axes of Fig. 4.

We further investigate the micro-magnetism in the compounds. Fig. 5(a) displays the ESR spectra for $Bi_{0.5}Sr_{0.5-x}Ba_xMnO_3$ ($x = 0$ and 0.20) at various temperatures. Clearly, only the paramagnetic (PM) signals with $g \sim 2$ have been detected in both samples. With decreasing temperature, the intensity of the PM signal increases first and reaches a maximum at a certain temperature, and then decreases. The above results indicate that the decrease of the intensity of the PM signal should be attributed to the transition from a PM/charge-disordered state to a charge-ordered state. In the temperature dependence of double-integrated intensities (DIN) as shown in Fig. 5(b), a remarkable peak appears at 490 K for $x = 0$ and 420 K for $x = 0.20$, which corresponds to the onset of charge